

# Constraints on the Scaling of the Mean Period of Ground-Motions using Inverse Random Vibration Theory

P. J. Stafford<sup>1</sup>, E.M. Rathje<sup>2</sup>

## ABSTRACT

The mean period of ground motions has a number of applications in both geotechnical and structural earthquake engineering. However, the most recent model developed to predict the distribution of mean period is over a decade old and makes use of discrete soil classes to capture linear site effects. This article presents a model for the influence of both linear and nonlinear site effects upon the mean period that is a function of the commonly used average shear-wave velocity. The model is developed by inferring the underlying Fourier amplitude spectra from the NGA West 2 models for response spectral ordinates using Inverse Random Vibration Theory and computing mean period values from these spectra. The developed model is valid over a broad range of magnitudes, distances and shear-wave velocities.

## Introduction

The mean period,  $T_m$ , of ground motions, first introduced by Rathje et al. (1998), has a number of uses within both geotechnical and structural earthquake engineering. In geotechnical applications, the mean period has been utilized for sliding block displacement predictions (Saygili and Rathje, 2008), slope stability and deformation (Stewart et al. 2003; Rathje and Antonakos, 2011) and the assessment of liquefaction potential (Athanasopoulos-Zekkos and Saadi, 2012). In the context of structural earthquake engineering, Kumar et al. (2011) demonstrated how the mean period was a useful predictor of demands for generic single and multiple degree of freedom oscillators, as well as for displacements and strength demands in steel moment resisting frames (Kumar et al., 2013a,b). In the above applications, the mean period is not used in isolation as a scalar intensity measure, but is rather used in conjunction with a measure of the amplitude of seismic demands in a vector. The work of Rathje et al. (2013) outlines the concepts and implementation requirements for such vector-framework approaches.

However, unlike many other commonly used intensity measures, very little attention has been paid to the development of predictive equations for the mean period. The notable exceptions to this point being the models of Rathje et al. (1998) and Rathje et al. (2004), with the latter being the most recent, and robust, model to have been published.

The model of Rathje et al. (2004) predicts the distribution of mean period as a function of magnitude and distance and incorporates the influence of site effects through discrete site class terms. In addition to generic source, path and site terms, Rathje et al. (2004) also model the effects of near-source directivity.

---

<sup>1</sup>Senior Lecturer, Civil & Environ. Engg, Imperial College London, London, UK, [p.stafford@imperial.ac.uk](mailto:p.stafford@imperial.ac.uk)

<sup>2</sup>Professor, Civil, Arch. & Environ. Engg, University of Texas at Austin, Austin, USA, [e.rathje@mail.utexas.edu](mailto:e.rathje@mail.utexas.edu)

When considering the many other intensity measures for which ground-motion models have been developed, the use of discrete site classes to represent the influence of near-surface sediments has almost ubiquitously given way to the use of the continuous parameter  $V_{S,30}$ , representing the time-averaged shear-wave velocity over the uppermost 30 m of material at the site. In addition, many ground-motion models for amplitude-based intensity measures have devoted significant attention to incorporating the influence of nonlinear site response.

Previous efforts to develop prediction equations for the mean period have made use of simple theoretical models for the Fourier amplitude spectrum of far-field shear waves that are described as a continuous function of frequency for input variables linked to the source, path and site. However, the representation of the site effects is not a function of  $V_{S,30}$  and this means that this numerical approach cannot be readily employed to constrain the scaling of the mean period with respect to this parameter. The purpose of the present article is to show how Inverse Random Vibration Theory (IRVT) can be used to develop a model for the effects of site response, both linear and nonlinear, upon the mean period of ground motions.

### **Definition of the Mean Period**

Following Rathje et al. (1998) and Rathje et al. (2004), the mean period is defined in terms of the ordinates of the Fourier amplitude spectrum of acceleration,  $A_i$ , at linearly-spaced frequencies,  $f_i$ , spanning the range  $0.25 \leq f_i \leq 20$  Hz and with a resolution of at least  $\Delta f \leq 0.05$  Hz. The particular expression is shown in Equation (1), from which it can be appreciated that the mean period is a weighted average of the period values over a pre-defined range with weights equal to the square of the Fourier acceleration amplitudes at these periods.

$$T_m = \frac{\sum_i A_i^2 (1/f_i)}{\sum_i A_i^2} \quad (1)$$

### **Inverse Random Vibration Theory**

It is clear that if one wished to develop a theoretical understanding for how the mean period should scale with respect to common seismological parameters then it is necessary to describe the Fourier amplitude spectrum of acceleration  $A(f)$  in terms of these parameters. However, the normal theoretical representation of the observed Fourier amplitude spectrum is written in terms of the linear product of source, path and site effects. Although this representation is very useful in many situations, it is not particularly helpful when the focus is upon the site effects. The reason for this is that whereas the source and path terms are conveniently written as continuous functions of frequency, simple analytical expressions do not exist for representing the effects of impedance contrasts associated with near surface layers (for all but the most simple of cases). As a result it is common to consider the influence of kappa, for which there is a very simple analytical expression, but to not attempt analytical representations for the amplification effects. In addition, the representation of the observed Fourier spectrum as a linear product of the source, path and site terms does not allow one to consider the effects of nonlinear site response.

In order to constrain the influence of linear and nonlinear site effects upon the scaling of the mean period IRVT is employed in this study. IRVT enables a consistent representation of the

Fourier amplitude spectrum to be obtained from an acceleration response spectrum (Gasparini and Vanmarcke, 1976; Kottke and Rathje, 2008). Therefore, if one applies IRVT to models for response spectra defined in terms of the average shear-wave velocity, and that also consider nonlinear site response, then it becomes possible to derive consistent Fourier amplitude spectra that reflect this nonlinear scaling and  $V_{S,30}$  dependence.

In this study, we apply IRVT to the recently released ground-motion models from the PEER NGA West 2 project (Abrahamson et al., 2014; Boore et al., 2014; Campbell and Bozorgnia, 2014; Chiou and Youngs, 2014). A very large number of scenarios were considered spanning a magnitude range from 4.2-8.0 (20 values), distances from 1-200 km (53 values logarithmically spaced), average shear-wave velocities from 150-1500 m/s (47 values logarithmically spaced), and three hypocentral depths. For all of these scenarios response spectra were computed using the NGA West2 models and then IRVT was applied. For each of the resulting Fourier spectra an estimate of the mean period was obtained. An example of the inverted spectra is shown in Figure 1 along with the resulting estimates of  $T_m$ . Note that the figure is plotted using a logarithmic abscissa but that the frequencies used in the Fourier transform are linearly spaced.

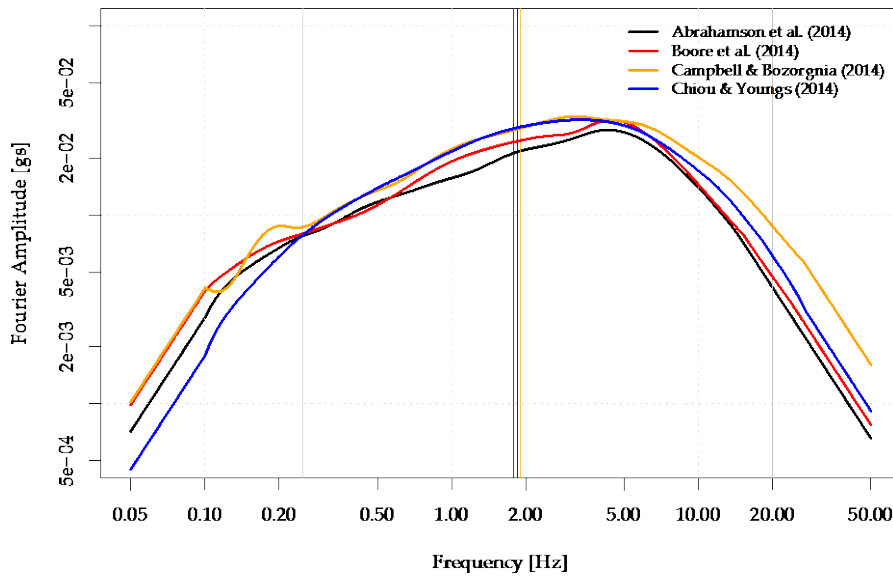


Figure 1. Example of inverted Fourier amplitude spectra using IRVT. The spectra shown are for a scenario  $M_w$  6 at  $R_{JB}$  10 km and a  $V_{S,30}$  of 760 m/s. The vertical grey lines represent the range considered for  $T_m$  calculations, while the coloured vertical lines show the  $T_m$  estimates.

### Functional Expression for Site Response

Although it is relatively straightforward to anticipate the scaling of the mean period with respect to magnitude and distance for generic rock conditions, through consideration of theoretical models for the Fourier spectra (Rathje et al. 2004), there is not a similarly simple way to infer analytical, or even numerical, scaling for the site effects. In particular, the representation of nonlinear site effects within the NGA West2 ground-motion models for response spectral amplitudes is already relatively complicated when individual response periods are considered

and our task here is to simultaneously represent the impact of these effects over a broad range of frequencies. The development of the functional form was therefore based entirely upon a combination of data exploration (with the ‘data’ in this case being the derived  $T_m$  values from the IRVT Fourier spectra – just under 150,000 scenarios for each of the considered NGA models) and conceptual understanding of how one should expect  $T_m$  to be impacted by both linear and nonlinear site response.

To constrain the linear site response we isolated the scenarios for which it is reasonable (and conservative) to expect that nonlinear site effects would not be relevant – this corresponded to all scenarios from events with magnitudes less than 5 and distances greater than 80 km (the maximum PGA values for these scenarios span 0.0035-0.0052 g for the NGA models). The NGA West2 models (with the exception of Campbell and Bozorgnia, 2014) also tend to use functional expressions that stop scaling the spectral amplitudes with respect to shear-wave velocity once the velocities exceed roughly 1100 m/s. For that reason the  $T_m$  values obtained from the IRVT process also will not scale with velocity over this range. All of the expressions for the site effects for  $T_m$  are therefore defined relative to values associated with velocities above 1100 m/s.

For all magnitude-distance scenarios we compute ratios of the inferred mean period values for all shear-wave velocity values with respect to the corresponding values for 1100 m/s. In the case that no effects of nonlinearity are present then these ratios should fall on top of one another for all considered magnitude and distance scenarios. Figure 2 demonstrates this behavior, along with the model predictions for linear site response that are represented by the functional expression shown in Equation (2). Note that the coefficient  $c_1$ , as well as other coefficients for the complete model are shown later in Table 1.

$$f_{LIN}(V_{s30}) = \ln \left[ T_m(V_{s30}) / T_m(V_{s30} = 1100) \right] = c_1 \ln \left[ \min(V_{s30}, 1100) / 1100 \right] \quad (2)$$

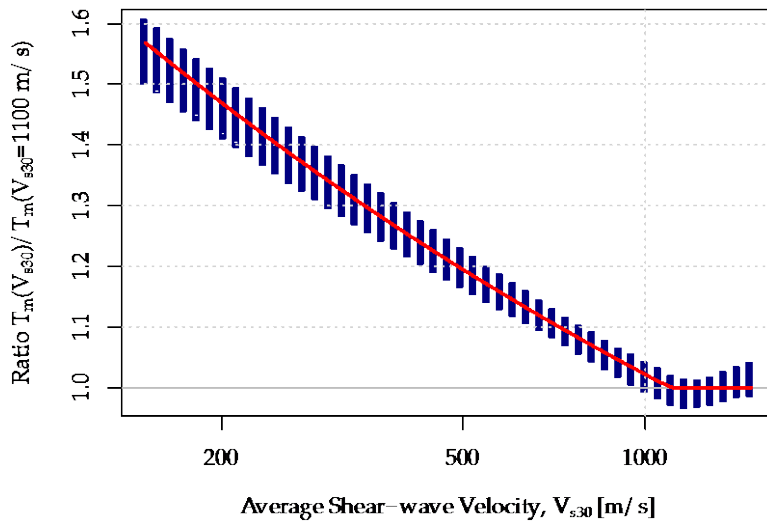


Figure 2. Ratios of mean periods for given shear-wave velocities for many magnitude-distance combinations. The model for linear site effects is shown by the red line.

It can be appreciated from Figure 2 that the model of Equation (2) performs very well over a broad range of shear-wave velocities. The slight increase in the dispersion for lower velocities reflects three phenomena: (1) that the figure shows ratios directly rather than their logarithms; (2) that the ratios have been anchored to the higher velocities; and (3) that the various NGA models have differences in their linear site response term that are larger at lower velocities.

To develop the nonlinear model all of the nearly 150,000 scenarios were considered simultaneously and rather than consider each NGA model individually, the ratios were developed using the mean of the period estimates from all of the previously reference NGA models, apart from Campbell and Bozorgnia (2014). We encountered some issues with obtaining consistent IRVT results from this particular model and as their site response terms are based upon the same source as the other models it was removed from the averaging.

Although the linear site effects scaled essentially linearly in the log-log space of the period ratio and shear-wave velocity, the scenarios for which nonlinear response was playing a role deviated significantly from this scaling. It was observed that there was an approximately exponential decrease in the logarithmic period ratios with respect to  $V_{S,30}$  but that the amplitude of the ratios for low velocities increased significantly with increasing magnitude and decreasing distance.

The expression adopted to model the remaining site effects is a function of the  $V_{S,30}$  as well as the magnitude of the event and the source-to-site distance. The terms involving the magnitude and distance are required to capture the effects of nonlinear site response and reflect the general scaling highlighted above. Again, it should be noted that this expression is entirely driven by the ‘data’ and has no theoretical basis. The expression for the nonlinear scaling is shown in Equation (3) with the values of the coefficients  $c_2$ - $c_6$  again shown in Table 1.

$$f_{NL}(V_{s30}) = \ln\left[T_m(V_{s30})/T_m(V_{s30} = 1100)\right] = \left[c_2 + c_3(M_w - 6)\right]\left[1 + c_4 \ln(R_{JB} + c_5)\right]\exp(-V_{s30}/c_6) \quad (3)$$

Table 1. Coefficients for Equations (2) and (3) – and hence Equation (4).

Coefficient	$c_1$	$c_2$	$c_3$	$c_4$	$c_5$	$c_6$
Value	-0.2258	2.3474	0.5257	-0.1318	3.6645	237.6582

This function performs well in cases where the nonlinear site effects are most dominant, at relatively short distances for moderate to large magnitude events, but for large distances predicts scaling that is inconsistent with linear site response. For that reason the final prediction equation is the larger of the predictions from Equations (2) and (3). The final model used to define the scaling of  $T_m$  with respect to hard rock sites ( $V_{S,30} > 1100$  m/s) is shown in Equation (4).

$$\ln\left[T_m(V_{s30})/T_m(V_{s30} = 1100)\right] = \max\left[f_{LIN}(V_{s30}), f_{NL}(V_{s30})\right] \quad (4)$$

The scaling of the data and the model predictions with respect to the shear-wave velocity are shown in Figure 3, for a number of distances and four separate magnitude values. Figure 4 shows a similar plot with respect to the Joyner-Boore distance, while Figure 5 shows the scaling with respect to magnitude for combinations of distance and shear-wave velocity.

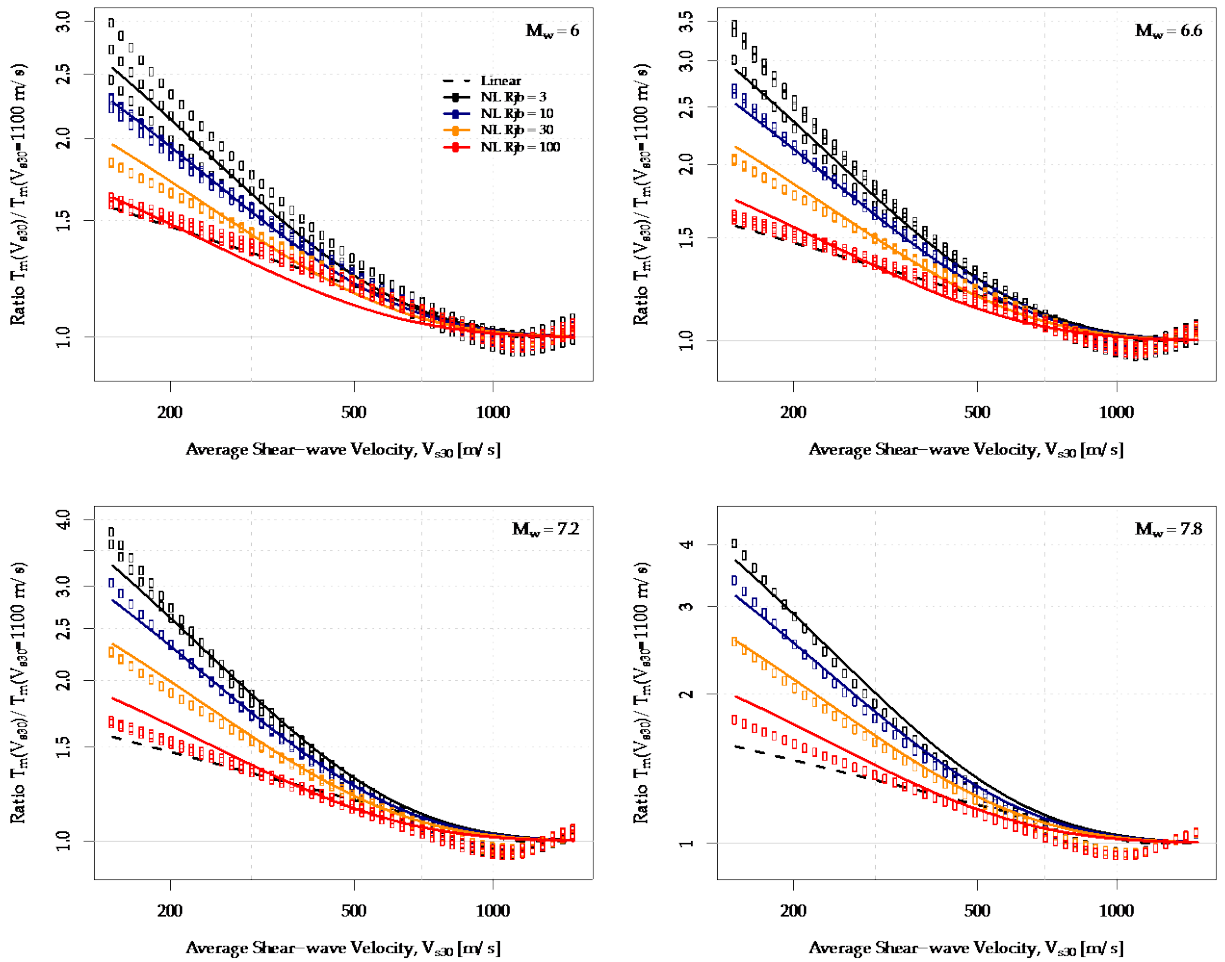


Figure 3. Scaling of the mean period ratios with respect to  $V_{S,30}$  for different  $M_w$  and  $R_{JB}$  values.

For the shortest distances and smallest magnitude values presented in both Figure 3 and Figure 4 it is possible to see a degree of dispersion in the inferred  $T_m$  values. This dispersion simply reflects the use of multiple depth values for the considered scenarios. All ruptures are assumed to be vertical strike-slip ruptures and for the large earthquakes considered the depth becomes irrelevant as all ruptures reach the surface whereas for the smaller events there are variable depths. These depths influence the degree of nonlinear site response that is implied by the NGA West2 models and hence impacts upon the inferred  $T_m$  values.

The dashed lines shown in Figure 3 and 4 represent the linear site effects predicted using Equation (2) and it can be appreciated that the nonlinear predictions (as well as some of the ‘data’) dip below these levels at large distances. While this was known during the model development, the focus was principally associated with ensuring that the model behaved reasonably well for the more severe scenarios associated with large demands and nonlinear site response. For all of the applications mentioned in the introductory section these more demanding scenarios are of most interest.

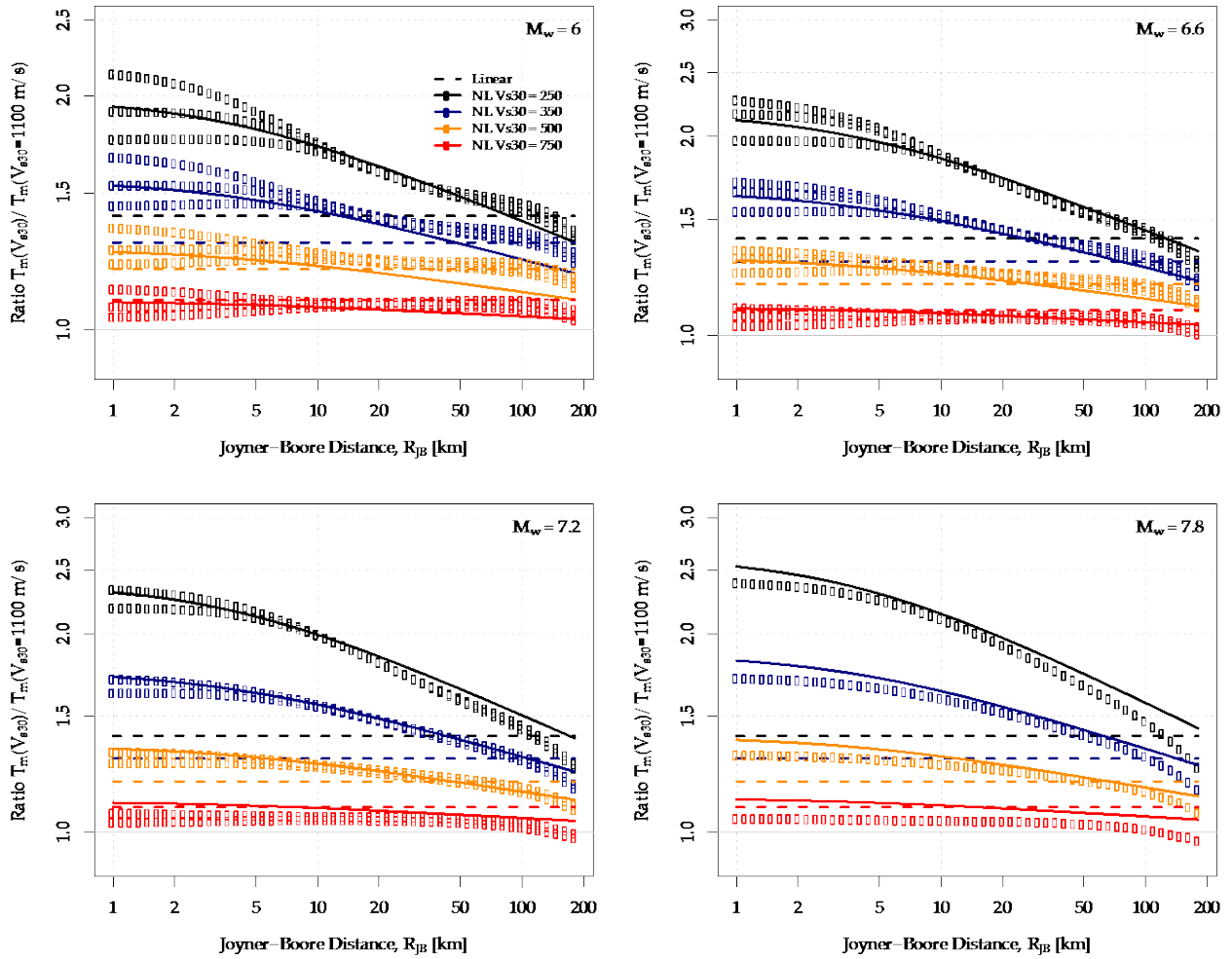


Figure 4. Scaling of the  $T_m$  ratios with respect to distance for a number of  $V_{s,30}$  and  $M_w$  values.

Figure 5 shows the scaling with respect to magnitude for a number of distance values which also demonstrates how the scaling of the nonlinear model breaks down to some extent for the largest considered distance. However, it can be appreciated that the scaling is generally well-captured.

Again, it should be noted that we are attempting to reflect the change of shape of the Fourier amplitude spectrum over a frequency range from 0.25 to 20 Hz, and hence a parameter derived from this spectrum, due to both linear and nonlinear site effects using just 6 coefficients. While there are clearly cases where our model does not predict the inferred period ratios perfectly, when judging the performance of the model it should be borne in mind that the NGA West2 models for the response spectra use significantly more coefficients for each period.

period. The existence of an updated model for the mean period should facilitate its consideration as an intensity measure within vector-based frameworks for seismic response analysis.

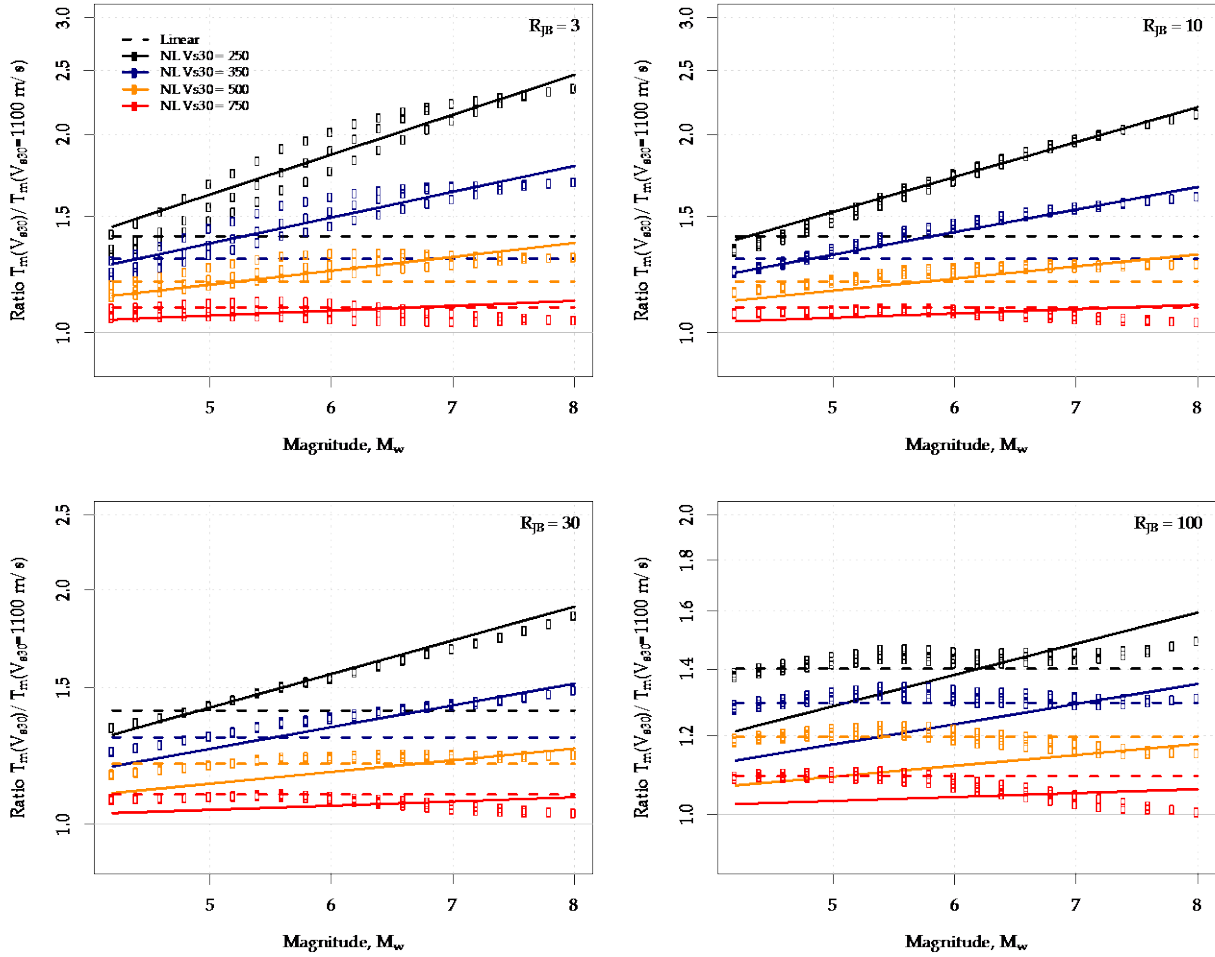


Figure 5. Scaling of the  $T_m$  ratios with respect to magnitude for a range of  $V_{s,30}$  and  $R_{JB}$  values.

## Conclusions

The presented model is able to capture the influence of site response upon the scaling of  $T_m$  in a robust manner given the relative simplicity of the model. The natural extension of the presented model is to embed this scaling for site response within a full predictive model for the mean

## References

- Abrahamson NA, Silva WJ, Kamai R. Summary of the ASK14 ground motion relation for active crustal regions. *Earthquake Spectra* 2014; **30**(3): 1025-1055
- Athanasopoulos-Zekkos A, Saadi M. Ground motion selection for liquefaction evaluation analysis of earthen levees. *Earthquake Spectra* 2012; **28**(4): 1331-1351
- Boore DM, Stewart JP, Seyhan E, Atkinson GM. NGA-West2 equations for predicting PGA, PGV, and 5% damped PSA for shallow crustal earthquakes. *Earthquake Spectra* 2014; **30**(3): 1057-1085
- Campbell KW, Bozorgnia Y. NGA-West2 ground motion model for the average horizontal components of PGA, PGV, and 5%-damped linear acceleration response spectra. *Earthquake Spectra* 2014; **30**(3): 1087-1115
- Chiou BSJ, Youngs RR. Update of the Chiou and Youngs NGA model for the average horizontal component of peak ground motion and response spectra. *Earthquake Spectra* 2014; **30**(3): 1117-1153

- Gasparini DA, Vanmarcke EH. SIMQKE: *Simulated earthquake motions compatible with prescribed response spectra*. Department of Civil Engineering Research Report R76-4. 1976. MIT.
- Kottke A, Rathje EM. *Technical manual for Strata*. PEER Report 2008/xx 2008. 95pp.
- Kumar M, Castro JM, Stafford PJ, Elghazouli AY. Influence of the mean period of ground motion on the inelastic dynamic response of single and multi degree of freedom systems. *Eq Engg & Struct. Dyn.* 2011; **40**: 237-256
- Kumar M, Stafford PJ, Elghazouli AY. Seismic shear demands in multi-storey steel frames designed to Eurocode 8. *Engineering Structures* 2013a; **52**: 69-87
- Kumar M, Stafford PJ, Elghazouli AY. Influence of ground motion characteristics on drift demands in steel moment frames designed to Eurocode 8. *Engineering Structures* 2013b; **52**: 502-517
- Rathje EM, Abrahamson NA, Bray JD. Simplified frequency content estimates of earthquake ground motions. *Journal of the Geotechnical Engineering Division ASCE* 1998; **124**(2): 150-159
- Rathje EM, Faraj F, Russell S, Bray JD. Empirical relationships for frequency content parameters of earthquake ground motions. *Earthquake Spectra* 2004; **20**(1): 119-144.
- Rathje EM, Antonakos G. A unified model for predicting earthquake-induced sliding displacements of rigid and flexible slopes. *Engineering Geology* 2011; **122**: 51-60
- Rathje EM, Wang Y, Stafford PJ, Antonakos G, Saygili G. Probabilistic assessment of the seismic performance of earth slopes. *Bulletin of Earthquake Engineering* 2013; doi: 10.1007/s10518-013-9485-9
- Saygili G, Rathje EM. Empirical predictive models for earthquake-induced sliding displacements of slopes. *Journal of Geotechnical and Geoenvironmental Engineering* 2008; **6**(1): 790-803
- Stewart JP, Blake TF, Hollingsworth RA. A screen analysis procedure for seismic slope stability. *Earthquake Spectra* 2003; **19**(3): 697-712